Biophysical Chemistry 150 (2010) 119–128

Contents lists available at ScienceDirect

Biophysical Chemistry

journal homepage: http://www.elsevier.com/locate/biophyschem

Effects of glycerol and urea on micellization, membrane partitioning and solubilization by a non-ionic surfactant

Hiren Patel, Gaurav Raval, Mozhgan Nazari, Heiko Heerklotz *

Leslie Dan Faculty of Pharmacy, University of Toronto, 144 College st, Toronto ON, Canada, M5S 3M2

ARTICLE INFO

Article history:
Received 12 January 2010
Received in revised form 18 March 2010
Accepted 18 March 2010
Available online 27 March 2010

Keywords:
Detergent
Osmolyte
Liposome
Isothermal titration calorimetry
Diphenylhexatriene
DLS

ABSTRACT

We have studied the effect of two cosolvents, urea and glycerol, on the association and interactions of a surfactant, octaethyleneglycol dodecyl ether ($C_{12}EO_8$) and a phospholipid (POPC). We have measured the CMC, the partition coefficient, the effective mole fractions X_e^{sat} and X_e^{sol} at the onset and completion of the membrane-to-micelle transition (membrane solubilization), and the enthalpies of transfer of surfactant by ITC. Changes in membrane order and dynamics were characterized by time-resolved fluorescence anisotropy measurements of DPH, and micelle sizes and clouding by light scattering. The cosolvents have complex effects that are not governed by the well-known 'salting in' or 'salting out' effects on the solubility alone. Instead, urea and glycerol alter also the intrinsic curvature ('effective molecular shape') of the detergent and the order and packing of the membrane. These curvature effects have an unusual enthalpy/entropy balance and are not additive for lipid and detergent. The results shed light on the phenomena governing lipid–detergent systems in general and have a number of implications for the use of cosolvents in membrane protein studies.

1. Introduction

The study of membrane proteins has become one of the key topics of biomedical research, and virtually all of these investigations require the use of detergents for the isolation of the protein from lipid membranes and its subsequent purification, characterization or reconstitution. Whereas the physico-chemical basics of lipid–detergent interactions in simple, binary systems are quite well understood (for reviews, see [1,2] and papers in Alonso and Goñi's special issue [3]), practical applications often require complex mixtures of detergents and cosolutes. In many cases, there are no suitable models to treat these multi-component systems and therefore, the technical procedures are developed and optimized on a largely empirical level. One example is Grisshammer's magical "triple detergent buffer" [4,5] which allows for the isolation and study of several G-protein coupled receptors (see also [6–8]) and comprises CHAPS, lauryl maltoside, cholesteryl hemisuccinate, 30 v% of glycerol, Tris, and NaCl. The success of this sophisticated system raises the questions why so many components are needed and what their functions are and their effects on protein, lipids, and co-solutes, respectively. We have started to tackle this problem by deriving and validating a model that describes the additive action of two or more detergents, such as CHAPS/LM, to solubilize a membrane [9]. Here we address the effect of glycerol and, for comparison, urea, on the self association, membrane partitioning, and membrane solubilization of non-ionic detergents. Further to its application upon membrane solubilization, glycerol is widely used to stabilize the native structure of globular proteins and to protect cells upon drying and freezing (including technical procedures as well as biological systems such as overwintering insects, etc.).

The effect of glycerol to stabilize the compact, native structure of globular proteins has been explained by several models, describing it as kosmotropic (a water-structure maker) and, according to Timasheff's concept [10,11], as preferentially excluded from the protein surface. This concept can be considered an application of Gibbs' adsorption isotherm (a macroscopic view of solute-induced changes in interfacial tension) at the molecular level: The minimization of free energy causes a solute that would increase the interfacial tension between two media (energetically unfavorable) to be preferentially excluded from this interface. This is the least of evils but the interfacial tension is, nevertheless, increasing due to the loss of mixing entropy in the interfacial region so that the system tends to minimize the interfacial area (e.g., of a protein by assuming a more compact state). MD simulations have provided detailed insight into the effect of glycerol on the composition, relaxation kinetics, and H-bonding of the solvation shell of a protein [12]. Specific details and extent of the interfacial effects depend on the molecular properties of the surfaces.

On a lipid membrane surface, the degree of exclusion of glycerol is even larger than adjacent to proteins [13]. This increases the interfacial tension of the membrane and favors structures with condensed interface. Koynova et al.'s [14] detailed model quantifies the resulting tendencies to freeze of a fluid bilayer into a gel phase [13,15] or convert it into an inverse hexagonal phase [15–17]. Based

* Corresponding author. Tel.: +1 416 978 1188; fax: +1 416 978 8511.
E-mail address: heiko.heerklotz@utoronto.ca (H. Heerklotz).

0301-4622/$ – see front matter © 2010 Elsevier B.V. All rights reserved.
doi:10.1016/j.bpc.2010.03.015

on the increased energy expense of exposing hydrophobic surface to water, one might expect glycerol also to promote the aggregation of a surfactant to micelles (i.e., a lowering of the CMC) or into a separate phase (i.e., a lower cloud point). While the prediction regarding the cloud point depression by glycerol was experimentally validated for $C_{12}EO_8$ [18], the CMCs of $C_{12}EO_8$ [18], Brij 58 (another EO-detergent), and CTAB [19] were found to increase upon addition of glycerol. This appears to indicate an anomaly of the EO-head group and/or glycerol; other kosmotropic cosolvents such as NaCl and sucrose decrease the CMCs of a series of surfactants as expected [20]. However, the fact that CMC-shifts do not scale with chain length also in these examples reveals a substantial impact of glycerol-head group interactions on the CMC. Particularly in case of EO-detergents, this seems to overcompensate the "salting out" of the chains. Controversial seems to be the issue whether the dehydration of the EO head group by glycerol renders the intrinsic curvature of a detergent less positive (thus promoting a lower interfacial curvature by a micellar growth to interconnected structures) [18] or, due to a collapse of the EO chain at the interface, more positive (causing the micelles to shrink) [19].

When it comes to detergent–lipid interactions, other kosmotropic additives like sucrose and NaCl increase the amount of octyl glucoside needed for complete membrane solubilization, which is quantified by the mole fraction X_e^{sol} (i.e., they reduce the capacity of its micelles to solubilize lipid). However, their effect on the onset of solubilization (X_e^{sat}) is weak and apparently complex [20]. No information seems available about the effect of glycerol on lipid–detergent interactions (including solubilization).

We compare the effects of glycerol on lipid–detergent systems with those of urea, a cosolvent that behaves just opposite to glycerol in most respects. Urea is a particularly prominent stabilizer of water-exposed surfaces that accumulates in interfaces (preferential interaction) and perturbs water structure (chaotropic effect). Hence, it promotes protein unfolding [11], demicellization [20,21], and inhibits surfactant clouding [21] by facilitating the exposure of hydrophobic surfaces to water. It stabilizes the fluid lipid bilayer with its relatively large interface and hydration against transitions to gel and inverse hexagonal phases [14,17,22]. By relaxing the interfacial tension of membranes it also renders otherwise detergent-resistant gel phases of long-chain saturated lipids susceptible for the insertion of Triton, followed by solubilization [23] and it reduces the amount of octyl glucoside that is required for complete membrane solubilization [20]. Urea has been used as a standard tool in (un)folding studies of globular proteins and there is evidence that also membrane protein stability can be modulated by urea [24].

To shed more light at the effect of glycerol and urea on lipid–detergent systems, we have studied their impact on the self-association (e.g., micelle formation), membrane partitioning, and membrane solubilization by $C_{12}EO_8$ and, in some cases, octyl glucoside (OG). All these phenomena can very precisely and conveniently be measured by isothermal titration calorimetry applying the demicellization [25–28], uptake and release [29], and solubilization and reconstitution [30] protocols. Fluorescence and light scattering data reveal the accompanying structural changes.

2. Materials and methods

2.1. Materials

Non-ionic detergents octaethyleneglycol mono-dodecylether ($C_{12}EO_8$) and n-octyl-β-$_D$-glucopyranoside (OG) were obtained from Anatrace Inc., Maumee, OH in Anagrade purity (99% HPLC). The lipid, 1-palmitoyl-2-oleoyl-*sn*-glycero-3-phosphocholine (POPC) was purchased from Avanti Polar Lipids, Alabaster, AL. Glycerol, a Bioshop Canada product with purity>99%, and Urea (99.5% purity) from Sigma-Aldrich were used without further purification. Diphenyl hexatriene (DPH) was from Molecular Probes (Invitrogen), Eugene OR. Solvents were prepared by mixing desired volumes of glycerol or weights of urea with water from a Millipore system. Volume fractions, ϕ can be converted into molar concentrations, C, according to (subscript U for urea, but eq. holds for glycerol analogously):

$$\phi = \frac{V_U}{V_{total}} = C_U\,\bar{V}_U \tag{1}$$

where V_U denotes the volume of urea added to the mixture of total volume V_{total}, C_U represents the molar concentration of urea, and $\bar{V}_U = 43.2$ mL/mol the partial molar volume of urea in aqueous solution. For glycerol we find $\bar{V}$ to range from ≈70.8 to 73.1 mL/mol for $\phi_G = 0$–1, respectively [31,32]. In other words, 1v% cosolvent corresponds to 0.23 M of urea or 0.14 M of glycerol, respectively.

2.2. Liposome preparation

Vesicles were prepared as described [29,30,33], simply replacing the buffer hydrating the dry lipid by one with the desired content of co-solvent. Briefly, a solution of POPC in chloroform was dried under a stream of nitrogen gas and under vacuum and the dry lipid film weighed and dispersed in the desired solution of glycerol or urea (0–40v%). Each suspension was vortexed and freeze-thawed for five cycles before large unilamellar vesicles (LUVs) of the desired diameter were prepared by extrusion through Nuclepore filters of ~100 nm pore size in a Lipex extruder (Northern Lipids, Canada). Spot checks of the final lipid concentration using an inorganic phosphorus assay (Biovision, Inc.) confirmed an effective molecular weight of POPC of about 778 g/mol (the formula weight is 760 g/mol, i.e., about one water molecule remains bound after drying) and ruled out a significant loss of lipid upon extrusion in water and urea/water. We assume this holds true also in glycerol/water where the assay failed to yield stable results. The size of LUVs was confirmed to be close to the pore size by dynamic light scattering.

2.3. Isothermal titration calorimetry

The measurements were performed using a VP isothermal titration calorimeter [34] produced by MicroCal Inc., Northampton MA applying the protocols explained below. In all cases, concentrations of titrant and original cell content during the titration were corrected for the displacement of some sample from the totally filled cell as detailed by the manufacturer. Injection volumes ranged between 2 and 15 μL and were, typically, increased during a titration to ensure optimum resolution at low titrant concentration while keeping the total time of the run acceptable. All experiments were done at 25 °C.

2.3.1. Demicellization protocol [25–27]

The injection syringe of the calorimeter was loaded with micellar dispersions of $C_D^{syr} = 3$ mM ($C_{12}EO_8$) or 500 mM (OG), respectively, in water–cosolvent mixtures of the desired composition. The cell was filled with the corresponding water–cosolvent mixture (same batch). The syringe content was titrated into the cell in a series of injections and the heat of re-equilibration of the cell content after each injection, Q_{obs}, was recorded as a function of the average detergent concentration in the cell during the respective injection, C_D. Typically, $Q_{obs}(C_D)$ shows a sigmoidal change from the concentration range below to that above the CMC, which is identified as the point of inflection (maximum or minimum of first derivative). The heat of demicellization, Q_{demic}, is estimated as the difference between the Q_{obs} curves below- and above the CMC, respectively, linearly extrapolated to the CMC (see Fig. 1 below for a graphical representation). Then, the molar enthalpy change of transfer of detergent from the aqueous solution into micelles, $\Delta H_D^{aq\rightarrow m}$, is calculated as:

$$\Delta H_D^{aq\rightarrow m} = -Q_{demic}\frac{C_D^{syr}}{C_D^{syr} - CMC} \tag{2}$$

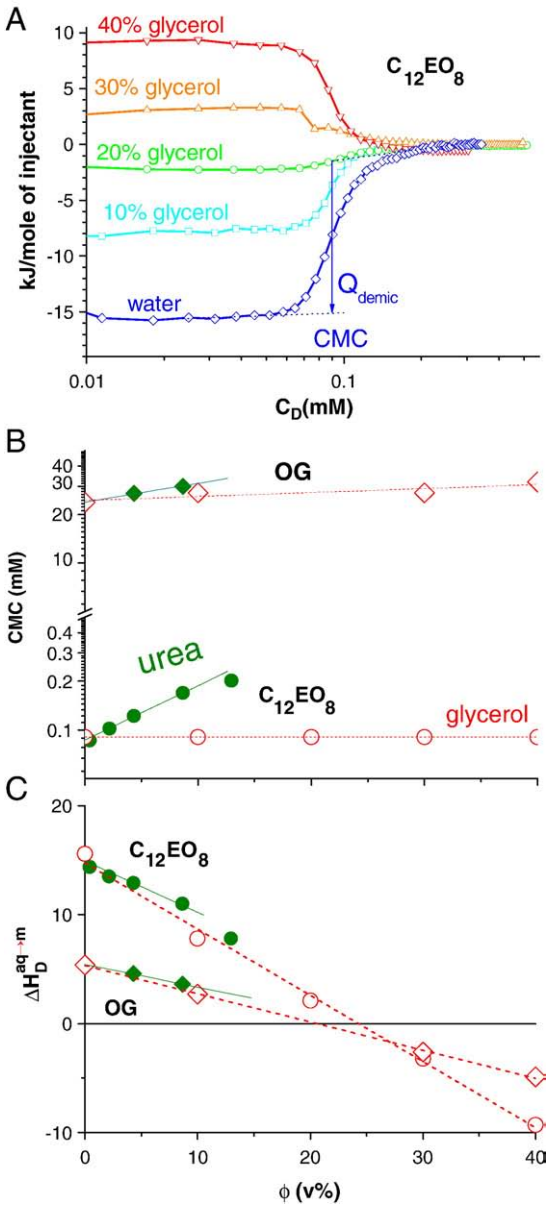

Fig. 1. Results of ITC demicellization experiments. Panel A: ITC demicellization curves as a function of the concentration of $C_{12}EO_8$ in the cell, repeated at a series of volume fractions of glycerol, at 25 °C. The arrow illustrates how the CMC and Q_{demic} are read from the plot by extrapolating pre- and post-transition base lines. Panels B and C compile the results for the CMC (notice log scale) and enthalpy of micelle formation for $C_{12}EO_8$ (circles) and OG (diamonds) as a function of urea (solid symbols) or glycerol (open symbols) content. The slopes of the linear regression lines (for urea limited to $\phi_U \leq 10$v%) yield the micellization parameters in Table 1.

by re-normalizing Q_{demic} from the total amount of detergent injected (concentration in syringe is C_D^{syr}) to the micellar detergent injected (concentration in syringe: C_D^{syr}-CMC). Note that $\Delta H_D^{aq\rightarrow m}$ and Q_{demic} refer to different directions of transfer and, hence, differ in sign.

2.3.2. Membrane partitioning characterized by uptake and release experiments [29,35]

A detailed step-by-step procedure can be found elsewhere [29]. Basically, for the uptake, the syringe is filled with a lipid vesicle suspension of C_L^{syr} and the cell is initially loaded with a detergent concentration well below the CMC (C_D^{ini}). For the experiments with $C_{12}EO_8$ described here, 50 μM and 25 μM of detergent were titrated with 15 mM lipid, respectively. In the release assay, the syringe is filled with vesicles that are pre-equilibrated with detergent (concentrations C_L^{syr}, C_D^{syr}) and the cell contains only the corresponding solvent. The data obtained from both types of experiments were evaluated using a global fit in a published spreadsheet [36] (problems of the macro buttons in Excel 2007 can be avoided by running the solver directly from the Data menu after proper installation of the Solver add-in).

2.3.3. Solubilization and reconstitution experiments

The main aim of these protocols is to establish the pseudo-phase boundaries at the onset and completion of membrane solubilization (i.e., detergent-induced membrane-to-micelle transition) which are specified here in terms of the critical mole fraction of the detergent in the aggregates, X_e^{sat} (onset) and X_e^{sol} (completion) [1,37]. All the membrane solubilization and reconstitution experiments were performed as described elsewhere [30]. For the solubilization experiment, the cell was filled with a 10 mM lipid vesicle suspension and these vesicles were titrated with a micellar solution of $C_{12}EO_8$ ($C_D^{syr} = 125$ mM). For the reconstitution assay, 40 mM of lipid was titrated into the cell loaded with 3 mM of $C_{12}EO_8$. These concentrations are high enough to render detergent monomers negligible to a good approximation, because $C_D \gg$ CMC and/or $C_L \gg 1/K$. Waiting times after each injection of 30 minutes were chosen because the equilibration (or achievement of a stationary state) may be slow in these systems. To enhance the resolution of the transfer enthalpy function at low solute concentration, the injection volumes were, typically, varied gradually from 0.7 to 15 μl.

2.4. Dynamic light scattering

DLS experiments were carried out in a Malvern Nano ZS (Malvern, Worcestershire, UK) utilizing non-invasive backscattering (NIBS) with a scattering angle of 173°. The light source is a He–Ne laser at 633 nm. Different parameters and algorithms were used to evaluate the results. Temperature-dependent changes in light scattering were monitored in terms of the derived count rate, i.e., the scattered intensity after correction for the individual attenuators used; this eliminates the effect of the temperature dependence of the viscosity on the data. Intensity-weighted size distributions at 25 °C were obtained by a multiexponential fit of the correlation function using the software provided with the instrument. Since the distributions are monomodal and largely symmetric, their maxima agree approximately with the z-average size of a cumulants analysis. DLS measurements at 25 °C were interpreted considering viscosities of 1.1 cP for 2 M urea and 2.64 cP for 30v% glycerol, respectively.

2.5. Fluorescence spectroscopy

For fluorescence measurements, diphenyl hexatriene (DPH) was mixed with the lipid in organic solvent at a 1:600 (DPH:POPC) mole ratio prior to drying and vesicle preparation in the respective solvent and dilution to 2 mM. Time-resolved anisotropy decays were recorded on a FL3 system (Horiba Scientific, Edison NJ) utilizing time correlated single photon counting. Excitation was realized by a 340 nm LED pulsed at 1 MHz, and emission was detected at 425 nm (slit 14.7 nm, double-grated monochromator) by a TBX detector. The software DAS6 (supplied by Horiba) was used for data evaluation.

3. Results

3.1. Micelle formation

Fig. 1 shows results of ITC demicellization experiments of $C_{12}EO_8$ at different concentrations of glycerol. Up to about 60 μM $C_{12}EO_8$ in water (blue, open diamonds in Fig. 1) in the cell, the instrument measures an almost constant, endothermic heat, Q_{obs} of ≈−16 kJ/mol arising, mainly, from the disintegration of the injected micelles. What is referred to as the CMC is, as usual, not a sharp boundary but the

midpoint of a rather broad transition range at about 60–120 μM with a point of inflection at 90 μM (defined here as the CMC). An arrow symbolizes the heat of demicellization and Eq. (2) gives $\Delta H_D^{aq\rightarrow m} = 15.6$ kJ/mol.

Addition of glycerol causes a dramatic change in Q_{demic} which vanishes between 20 and 30% glycerol and then turns positive whereas the CMC remains almost constant (see also open circles in Fig. 1C). However, in contrast to what one might expect for a preferentially excluded cosolvent, the CMC of both $C_{12}EO_8$ (Fig. 1 A, open circles in 1B) and OG (open diamonds in 1B) is virtually unchanged by glycerol up to 40v%. Aramaki [18] published a slightly larger CMC of 109 μM in water and a moderate increase to 146 μM at 40v% glycerol. One reason for somewhat different CMC values obtained by different methods is the considerable width of the transition which is disregarded by the phase model of micellization, causing some ambiguity in defining the CMC in the first place. Urea increases, as expected, the CMC of $C_{12}EO_8$ and OG (solid symbols in Fig. 1B) but decreases their micellization enthalpies (solid symbols in 1C) almost identically as glycerol.

Considering solution and micelles as two pseudo-phases, we may derive the standard chemical potential difference of micelle formation:

$$\Delta\mu_D^{0,aq\rightarrow m} = -RT\ln\left[\frac{C_D^{0,aq}}{CMC}\right] \tag{3}$$

where $C_D^{0,aq}$ denotes the concentration of the detergent in solution representing its standard state, where its activity becomes 1. Here, it is most suitable to choose a 1 M solution, i.e., $C_D^{0,aq} \equiv 1$ M. The slopes of $\Delta\mu_D^{aq\rightarrow m}$ and $\Delta H_D^{aq\rightarrow m}$ as a function of ϕ are compiled in Table 1 below.

3.2. Membrane partitioning

Fig. 2A illustrates the global fit of uptake and release experiments to determine the partition coefficient, K, and the enthalpy of transfer, $\Delta H_D^{aq\rightarrow b}$, of $C_{12}EO_8$ from the aqueous phase including, in this example, 0.5 M (=2.2 v%) of urea into bilayers. The uptake of detergent monomers from solution in the cell into vesicles injected from the syringe is endothermic. In this assay, the heats decrease in the course of the titration because less and less detergent remains free and able to partition into newly added liposomes. The release of pre-bound detergent upon injection of a small aliquot of mixed lipid–detergent liposomes into an excess of buffer in the calorimeter cell is exothermic, because the reversion of the direction of the transfer changes the sign of the heat of transfer. As detailed elsewhere, a global fit of several uptake and release curves has major advantages [29]. One shared fit parameter is the membrane–water partition coefficient, K, defined here on the basis of the mole ratio:

$$K \equiv \frac{C_D^b}{C_L C_D^{aq}} = \frac{R_e}{C_D^{aq}} \tag{4}$$

where C_D^b denotes the molar concentration of bilayer-bound detergent (referred to the total volume of the dispersion), C_L is the lipid concentration (all lipid is in aggregates, here: liposomes), and C_D^{aq} stands for the concentration of 'aqueous' (here: incl. co-solvents) detergent monomers. The second equality illustrates that C_D^b/C_L is just R_e, the effective mole ratio of 'bound' detergent to lipid. Other fit parameters are the molar enthalpy of detergent transfer from solution into the bilayer, $\Delta H_D^{aq\rightarrow b}$ (shared), and a constant term usually referred to as heat of dilution, Q_{dil}, which, however, comprises also

Table 1
Derivatives of standard free energy and enthalpy changes of transfer of $C_{12}EO_8$ with respect to the volume fraction of glycerol and urea, respectively. Values and errors are derived from slopes and standard errors of linear fits (additional errors may apply) of data in Fig. 2 (for aq→m, aq→b; using $d\Delta\mu^0/d\phi = -RT\,2.3\,d(\log K)/d\phi$) and Fig. 4 (for m→b), respectively.

Y	dY/dϕ in kJ/(mol v%)	
	Glycerol	Urea, $\phi \le 0.1$
OG		
$\Delta\mu_D^{0,aq\rightarrow m}$	0.014 ± 0.005	0.06 ± 0.01
$\Delta H_D^{aq\rightarrow m}$	-0.26 ± 0.01	-0.21 ± 0.01
$C_{12}EO_8$		
$\Delta\mu_D^{0,aq\rightarrow m}$	0.00 ± 0.01	0.19 ± 0.01
$\Delta H_D^{aq\rightarrow m}$	-0.61 ± 0.03	-0.47 ± 0.07
$\Delta\mu_D^{0,aq\rightarrow b}$	0.01 ± 0.01	0.22 ± 0.03
$\Delta H_D^{aq\rightarrow b}$	-0.7 ± 0.2	-0.1 ± 0.4
$\Delta\mu_D^{0,m\rightarrow b}$	-0.011 ± 0.003	0.021 ± 0.005
$\Delta\mu_L^{0,m\rightarrow b}$	$+0.004 \pm 0.003$	0.03 ± 0.01
$\Delta H_D^{m\rightarrow b}(R_e\rightarrow 0)$	-0.15 ± 0.02	Nonlinear
ρ_H^0	-0.19 ± 0.03	Nonlinear

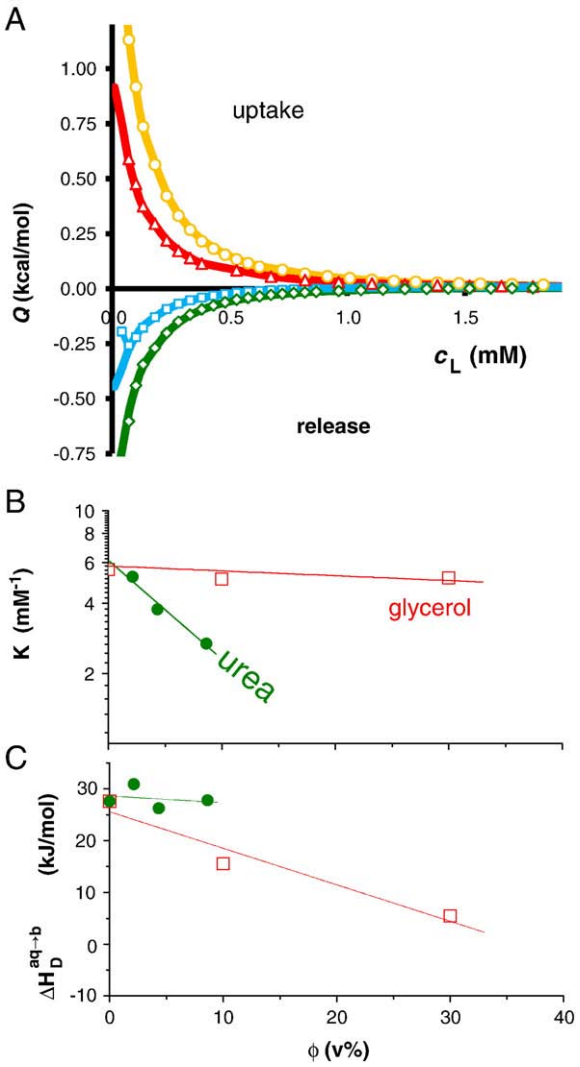

Fig. 2. Uptake and Release profile showing normalized reaction heats, Q, versus lipid concentration in the presence of 0.5 M urea. The data (A) refer to uptake titrating 15 mM POPC into 50 μM (circles) and 25 μM (triangles) of $C_{12}EO_8$ and release experiments titrating mixed vesicles comprising 15 mM POPC and 1 mM (squares) or 2 mM (diamonds) of $C_{12}EO_8$ into buffer. The curves represent a global fit with the shared parameters K=5.2/mM, $\Delta H_D^{aq\rightarrow b}$=7.5 kJ/mol, γ=1 (both membrane leaflets are accessible to detergent), and individual, small values of Q_{dil} . Panels B, C show K (note log scale) and $\Delta H_D^{aq\rightarrow b}$ as a function of the volume fraction, ϕ, of urea (solid circles) and glycerol (open squares) in water at 25 °C.

'blank' heats resulting from other effects such as the imperfection of the temperature match between injectant and cell, mechanical work of injection, etc (individual). All fits are in line with the assumption that the detergents flip-flop quickly between the inner and outer leaflet of the bilayer so that all lipid is accessible for partitioning and the 'accessibility parameter', $\gamma = 1$ [29,38].

Fig. 2B, C shows that both urea and, much less so, glycerol decrease K, i.e., they stabilize detergent in solution compared to the membrane-inserted state. Urea has very little effect on the enthalpy of transfer but glycerol renders it less endothermic, qualitatively similar to the enthalpy of micellization. Again, the slopes of the lines in Fig. 2 are considered in Table 1, with the standard chemical potential change, $\Delta\mu_D^{0,aq\to b}$, obtained as:

$$\Delta\mu_D^{0,aq\to b} = -RT\ln\left(K \times C_D^0\right) \tag{5}$$

choosing a standard state of a solution of $C_D^0 = 1$ M.

3.3. Membrane solubilization and reconstitution

Membrane solubilization is usually well described by Helenius and Simons' [39] 3-stage model, according to which a system encounters with increasing detergent content the following stages: (i) detergent binding, (ii) lamellar–micellar phase transition, and (iii) size decrease of mixed micelles. If the detergent concentration is specified in terms of the effective, local mole fraction within aggregates, X_e:

$$X_e = \frac{C_D^b + C_D^m}{C_L + C_D^b + C_D^m} + \frac{C_D - C_D^{aq}}{C_L + C_D^b + C_D^m} \tag{6}$$

the onset and completion of solubilization (the lower and upper boundary of stage 2) can be assigned to values denoted X_e^{sat} and X_e^{sol}, respectively, that are characteristic for a given detergent–lipid pair and temperature and do not depend on absolute concentrations etc. The concept was introduced for mole ratios [37], $R_e = X_e/(1-X_e)$, but fractions are more convenient here.

A uniquely simple, convenient and precise means of establishing X_e^{sat} and X_e^{sol} is to cross these boundaries in one or more ITC experiments, either by titrating detergent micelles into a liposomal dispersion of lipid (solubilization experiment) or vice versa (reconstitution experiment) [30,40]. The absolute concentrations of the titrant at the phase boundaries are indicated as sudden changes of the heats of titration, in most cases involving actually a change in sign (Fig. 3). For $C_{12}EO_8$ in the different solvents studied here, the partition coefficient is sufficiently large ($K \geq 2.6$/mM) to ensure that at 10 mM lipid used for the solubilization assays, >96% of the detergent are bound to aggregates. Reconstitution experiments were done well above the CMC of the detergent. We can therefore obtain the effective fractions directly from the break points of the ITC curves on the total mole fraction scale, $X_e^{sat} = X^{sat}$ and $X_e^{sol} = X^{sol}$, to a very good approximation. Furthermore, we may approximate $\Delta H_D^{m\to b}(X<X^{sat}) \approx Q_{obs}(X)$ of the solubilization experiment, at least except for the first few injections. In Fig. 3, this range is fitted by a blue, dashed model curve according to:

$$Q_{obs}(X) = \Delta H_D^{m\to b}(0) + \rho_H^0\left[(1-X)^2 - 1\right] \tag{7}$$

which has been derived analogously to the model of regular solutions yet with the important difference that we assume quasi-random mixing but do not exclude intramolecular entropy changes so that the non-ideality parameter for the mixing enthalpy, ρ_H^0, does not agree with the non-ideality parameter for the free energy [41].

Fig. 3B reveals that urea reduces X_e^{sat} and X_e^{sol} of $C_{12}EO_8$, i.e., it destabilizes the mixed membrane and promotes its solubilization to micelles. Glycerol has a very weak, membrane-stabilizing effect. The

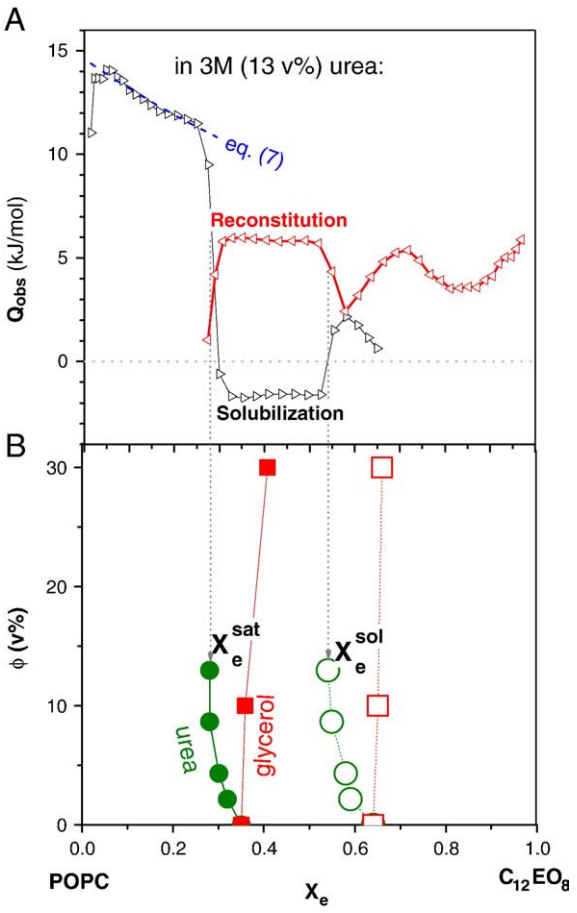

Fig. 3. Results of ITC solubilization and reconstitution experiments. Panel A shows observed heats, Q_{obs}, of a solubilization (right-pointing triangles) and a reconstitution experiment (left-pointing triangles) with $C_{12}EO_8$/POPC in 3 M urea at 25 °C as a function of the mole fraction of detergent in the aggregates, X_e. The blue dashed curve in A illustrates a fit according to Eq. (7), yielding $\Delta H_D^{m\to b}(0)$ and ρ_H^0 as plotted in Fig. 4C. The boundaries of the bilayer-to-micelle transition range, X_e^{sat} and X_e^{sol} are marked and included in panel B. B compiles values of X_e^{sat} (solid symbols) and X_e^{sol} (open symbols) as a function of the volume fraction, ϕ, of urea (circles) or glycerol (squares), respectively.

enthalpy changes, expressed in terms of $\Delta H_D^{m\to b}(0)$ and ρ_H^0 are plotted in Fig. 4C.

The standard chemical potential of transferring a non-ionic detergent from a micelle into a bilayer can be derived as [42]:

$$\Delta\mu_D^{0,m\to b} = -RT\ln\frac{X_D^b}{X_D^m} = -RT\ln\frac{X_e^{sat}}{X_e^{sol}}, \tag{8}$$

taking into account that the compositions at the phase boundaries are just those of the coexisting bilayers and micelles, $X_e^{sat} = X_D^b$ and $X_e^{sol} = X_D^m$. For the lipid, we find with $X_L^m + X_D^m = 1$ (and analogously for bilayers) that:

$$\Delta\mu_L^{0,m\to b} = -RT\ln\frac{X_L^b}{X_L^m} = -RT\ln\frac{1-X_e^{sat}}{X_e^{sol}}. \tag{9}$$

These transfer potentials are shown below in Fig. 4 A,B.

3.4. Micelle size distribution and cloud point

Fig. 5 illustrates the effects of cosolvents and temperature on the size of $C_{12}EO_8$ micelles as detected by light scattering. The intensity of back-scattered light in terms of derived count rates (=real count

rates times attenuation factor of the attenuator) illustrates the temperature-induced changes of micelle size dispersions in the different solvents. At the cloud point (at the upper temperature limit of the curves shown in Fig. 5A), the scattered light intensity increases very steeply and becomes unstable over time (after true phase separation, the sample is cleared). Glycerol shifts the cloud point to lower temperatures and appears to reduce the temperature range of micellar growth preceding clouding. Urea shifts T_C to higher temperature and seems to facilitate a more gradual growth of the micelles. These effects are in line with the expected salting out and salting in phenomena caused by glycerol and urea, respectively.

While scattering intensities are the most robust parameter to illustrate temperature effects, they do not permit a comparison of micelle sizes between the different solvents at a given temperature because the solvents differ in refractive index. To this end, Fig. 5B shows the intensity-weighted distributions of the hydrodynamic radii of the micelles at 25 °C. Micelles of $C_{12}EO_8$ in water show a broad size distribution which comprises non-spherical shapes with R_H substantially bigger than the maximum length of a molecule, ≈4.5 nm. Naively, one might expect urea and glycerol to have opposite effects on micelle size but both are found to induce a down-shift and narrowing of the intensity-weighted size distribution (see below for discussion).

3.5. The effects of cosolvents on the time-resolved fluorescence anisotropy of DPH

Fig. 6 shows the results of time resolved fluorescence anisotropy measurements with DPH (mole ratio to POPC 1:600). The anisotropy decays for vesicles prepared in 2 M urea (green) and 30v% glycerol were fitted by a monoexponential decay

$$r(t) = (r_0 - r_\infty)\exp\left\{-\frac{t}{\theta}\right\} + r_\infty. \quad (10)$$

The rotational correlation time θ is in the range of several ns (representing the dynamics of the probe) and the limiting anisotropy r_∞ (quantifying the constraints to its motion, i.e., order) is very small yet not zero. These parameters are plotted in Fig. 6 B,C as a function of temperature.

The results support the hypothesis that exposure of the membrane to 30% glycerol condenses its lateral packing, thus slowing down rotational motion and increasing order, particularly at low temperature. However, these effects are weak. At room temperature, 30% glycerol slow down DPH dynamics similarly as a decrease in temperature by of the order of 6 K (ratio 0.2 K/v%).

While the results for glycerol were in line with the expectation for a salting-out cosolvent, the lack of an effect of urea to disorder the chains and accelerate their dynamics (2 M, not shown, and 3 M, Fig. 6) is surprising considering its activity to promote the gel-to-fluid transition and facilitate the exposure of hydrophobic surface to water. The finding is, however, in accord with other studies reporting, for example, urea to replace water under low-humidity conditions but to have little effect on membranes in excess water [43] and with other experiments in our study showing that urea effects on membranes cannot be explained in terms of surface activity or salting in alone.

4. Discussion

4.1. Cosolvent effects, m-values

Table 1 lists the slopes of the effects of the cosolvents on the standard chemical potentials and enthalpies of transfer as obtained from demicellization (Fig. 1), partitioning (Fig. 2), and solubilization (Fig. 4) experiments. On the first glance, we notice that (i) the transfer potentials fulfill, within error, the requirement to be independent of the pathway, e.g.:

$$\Delta\mu_D^{0,aq\to m} + \Delta\mu_D^{0,m\to b} = \Delta\mu_D^{0,aq\to b}; \quad (11)$$

note that the absolute errors of the partitioning data are larger. (ii) We see that the enthalpy changes are more than an order of magnitude larger than the respective chemical potential differences, illustrating that the effects governing our systems and processes are subject to almost perfect enthalpy-entropy compensation. (iii) If the effects of urea and glycerol could all be explained in terms of chaotropic and kosmotropic effects, respectively, the effects of glycerol and urea should be opposite and the values within each row should differ in sign. This is not the case; instead, we have to consider a number of competing phenomena as explained in the following sections.

The effect of urea on the thermodynamic parameters assessed here is not always linear and in some cases not even monotonic, this has been described for micellization before [44]. Table 1 gives approximate slopes fitted in the range up to 10v% but this does not exclude moderate, systematic deviations from linearity even in this concentration range. It should be noted that the slopes in Table 1 can be converted into the unit of cal/(mol M) for comparison with so-called m-values quantifying denaturant effects on protein stability. For urea, $m = (dY/d\phi)\times 4.32\text{v\%/M}\times 239$ cal/kJ, for glycerol: $m = (dY/d\phi)\times 7.2\text{v\%/M}\times 239$ cal/kJ.

4.2. Solvent effects on alkyl chains in solution

As outlined in the introduction, a primary effect of cosolvents is to change the free energy of the interface between the molecule (primarily the alkyl chain) and the solvent. Macroscopically, the contribution of an interface to the free energy of the system can be written as γA, where A stands for the interfacial area and γ for the interfacial tension. For discrete molecules at molecular (and hence rough) surface, we may formally write

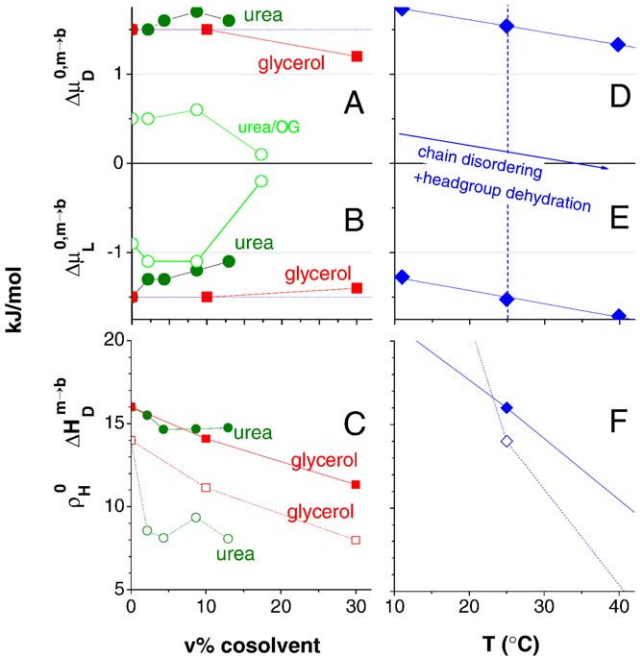

Fig. 4. The standard chemical potential differences of transfer of lipids (A and D) and detergents (B and E) and the enthalpy of micelle-to-bilayer transfer at $X_e \to 0$ ($\Delta H_D^{m\to b}$ (0), open symbols in C and F) and enthalpic non-ideality parameter (ρ^0_H, solid symbols in C and F) as a function of cosolute content (A, B and C, green circles for urea and red squares for glycerol) and temperature D, E and F (values from [42]). All points are for $C_{12}EO_8$ except for the green open circles in A and B representing Walter et al.'s [20] data for OG. Ordinates of right panels are chosen to match those of the left ones, the abscissae are related by 1 K/v%, respectively. (For interpretation of the references to color in this figure legend, the reader is referred to the web version of this article.)

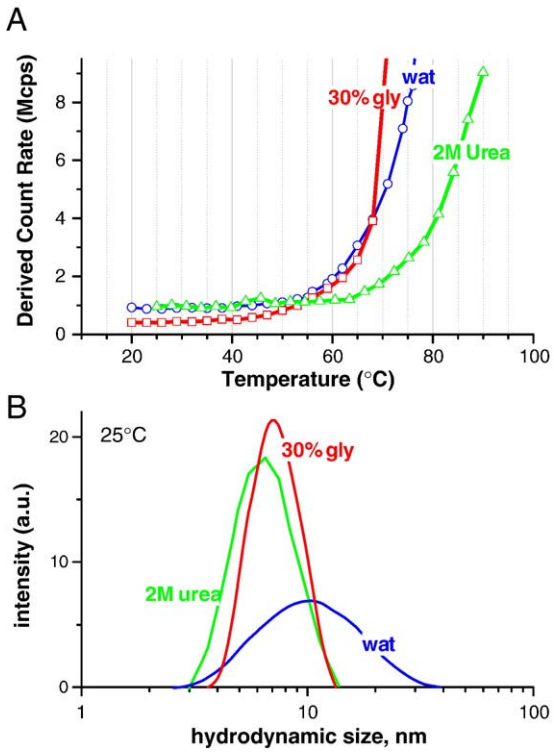

Fig. 5. Results of light scattering experiments with micelles of $C_{12}EO_8$ in different solvents. Panel A displays the scattered light intensity of the micelles (10 mM $C_{12}EO_8$) in water (spheres, blue), water with 2 M urea (triangles, green), and water with 30v% glycerol (squares, red) as a function of temperature. Clouding is indicated by a virtually vertical increase at the end of the curves. Panel B shows intensity-weighted size distributions of these micelles at 25 °C as obtained by DLS. The arrow indicates the approximate length of a stretched $C_{12}EO_8$ molecule which represents an upper limit of R_H of a spherical micelle. (For interpretation of the references to color in this figure legend, the reader is referred to the web version of this article.)

the interfacial energy as $\gamma_e \times$ ASA. Here, ASA stands for the solvent accessible surface area and γ_e for an effective interfacial tension (which is not necessarily identical with the macroscopic γ, for details, see [45]). By preferential interaction with the molecular surface, urea reduces the interfacial tension by $\delta\gamma_e$ and the reduction of $\mu_D^{0,aq}$ by $\delta\gamma_e \times$ ASA will increase the CMC and decrease K by the same factor, contributing equally to $d\Delta\mu_D^{0,aq\rightarrow m}/d\phi_U$ and $d\Delta\mu_D^{0,aq\rightarrow b}/d\phi_U$ (see Table 1). Furthermore, the effect of $\delta\gamma_e$ should scale with ASA, i.e., by larger for $C_{12}EO_8$ than for the smaller OG, for example.

Inspection of our results reveals that urea does, indeed, decrease −ln CMC and ln K of $C_{12}EO_8$ to a similar extent and that −ln CMC of OG decreases less steeply than of $C_{12}EO_8$. The ratio between $d\Delta\mu_D^{0,aq\rightarrow m}/d\phi_U$ for $C_{12}EO_8$ and OG, ≈2.5, is somewhat larger than the ratio between the ASA of the dodecyl and octyl chains, ≈1.5. For a more quantitative comparison, let us convert the urea effect on micelle formation to an m-value of +170 cal/(mol M). Assuming that micellization keeps the head group exposed to the solvent and with an upper limit of ΔASA for a lauryl chain of ΔASA<650 Å^2 [46], we obtain m>0.26 cal/(mol M)×ΔASA_{np} (subscript 'np' for nonpolar). This is at or above the upper level of m values induced by ΔASA_{np} upon protein denaturation, m=[(0.15±0.12) ΔASA_{np}+0.08 ΔASA_{pol}] cal/(mol M Å^2) [47]. Summarizing, we may conclude that the effect of urea on the CMC and (for $C_{12}EO_8$) on K is largely (yet not exclusively) governed by the "salting in" of the detergents, i.e., the stabilization of the detergents in solution. This may also account for the increase in the cloud point of $C_{12}EO_8$ caused by urea.

For glycerol as a preferentially excluded cosolvent, $\delta\gamma_e$>0 (this effect is even stronger for membranes than for proteins [13]). That means, one may expect all phenomena discussed in the previous paragraph to be reversed compared to urea, if the glycerol system is governed by the analogous phenomena. However, instead of decreasing, the CMC is unaffected or even slightly increased by glycerol (see also [18]), indicating that it is not governed by $\delta\gamma_e$ and the calculated maximum ASA of the chain.

The strong changes of the enthalpies of micellization and partitioning induced by the cosolvents including a change from endothermic to exothermic values are strongly reminiscent of the temperature dependence of the transfer enthalpies. The slopes of the latter are just the heat capacity changes, which is $\Delta C_P = -600$ J/(mol K) for $C_{12}EO_8$ micellization [42]. Correlating ΔC_P with $d\Delta H_D^{aq\rightarrow m}/d\phi$ yields a ratio of ≈1 K/v% for $C_{12}EO_8$/glycerol. For OG, we obtain a somewhat smaller ratio of 0.74 K/v% with $\Delta C_P = -350$ J/(mol K) [27]. Cosolvent-induced changes of the interfacial free energy of solvent-exposed detergent molecules explain also the shifts in the cloud point of $C_{12}EO_8$.

4.3. Head group interactions, chain order, and curvature stress

Whereas the free energy change upon detergent self association and membrane partitioning (and, consequently, CMC and K) are dominated by the hydrophobic effect (previous section), the remaining ASA in micelles and membranes is relatively small and similar. Instead, the most important difference between micelles and membranes is their different interfacial curvature and packing (at least for non-ionics). Detergents form micelles because their hydrated head group occupies a lateral interface area that is larger than the area

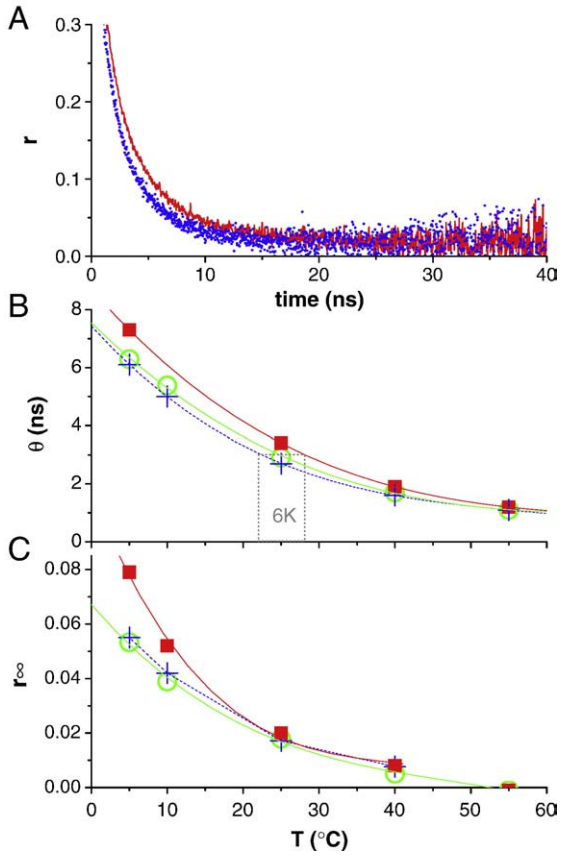

Fig. 6. Effects of cosolvents on membrane dynamics and order as indicated by DPH time-resolved anisotropy. A: Anisotropy decays of DPH, 1:600 mol in POPC vesicles (2 mM) in water (blue dots) and water + 30v% glycerol (red line) at 25 °C. The temperature (T) dependence of the rotational correlation times of DPH (θ, B) and minimum anisotropy (r_∞, C) for vesicles made in water (blue crosses), 3 M urea (ϕ_U = 13%) (green open circles) and 30v% glycerol (red squares). (For interpretation of the references to color in this figure legend, the reader is referred to the web version of this article.)

needed by the hydrophobic part. This 'inverted cone-like effective shape' [48,49] causes the detergent to prefer a curved interface of a radius $R = 1/c_0$; c_0 is referred to as the intrinsic curvature [50,51]. Micelles can, typically, adapt their size and shape to establish a real interfacial curvature that matches the intrinsic curvature, c_0, of their constituents. There is, however, a gap between the minimum curvature in a micelle and the on average, non-curved topology of a membrane interface. When detergents with $c_0 > 0$ insert into a membrane, they cause a curvature stress that contributes a penalty of $\kappa c_0^2/2$ to the free energy per area of the membrane [50,51] (κ is the bending rigidity of the membrane leaflet). In other words, the standard free energy of transfer of a detergent from a rather stress-free micelle into a bilayer, $\Delta\mu_D^{m\to b}$ (see Fig. 4), represents approximately the curvature stress in the membrane. It is noteworthy that for small X_e^{sat}, one finds that $\Delta\mu_D^{m\to b} \approx -RT\ln(K\times CMC)$ so that the product $K\times CMC$ allows to tell strong curvature stress inducers ('strong detergents', $K\times CMC > 1$) from weak ones [52]. Andelman et al. [50,53] have established a sophisticated quantitative model of membrane solubilization on the basis of intrinsic curvatures.

Before we discuss the consequences of urea and glycerol on c_0 as a clue to understand their effect on solubilization, let us illustrate the molecular strains that result from c_0 in a membrane in terms of its temperature dependence. Increasing temperature tends to dehydrate the head groups and to disorder the chains. Both effects reduce the curvature strain in the membrane and, hence, shift the structural preferences in favor of bilayers. The dehydration of the head groups makes them smaller and renders the effective shape of the molecules less cone-like. The disordering of the chains expands the effective area per chain (at the expense of membrane thickness) so that it tends to catch up with head group size and c_0 decreases. Furthermore, disordering and thinning are also expected to reduce the bending stiffness κ of the leaflet, further decreasing curvature strain. The sum of all these effects is indicated by virtually identical, positive, slopes of $d\Delta\mu_D^{0,b\to m}/dT = 14$ J/(mol K) and $d\Delta\mu_L^{0,b\to m}/dT = 15$ J/(mol K) for $C_{12}EO_8$ [42] (Fig. 4 D, E). Because curvature stress-induced disordering perturbs chain–chain interactions but increases the conformational entropy of the chain, its impact on free energy is subject to strong, almost complete enthalpy–entropy compensation. Hence, it is much more sensitively revealed by enthalpy changes (see Fig. 4F) with $\Delta H_D^{m\to b}(0)$ reflecting the misfit of an isolated detergent with the membrane geometry (i.e., its intrinsic curvature) and the non-ideality parameter ρ_H^0 illustrating the detergent-induced disordering of the membrane (reducing the enthalpic penalty upon further detergent uptake).

4.4. Glycerol increases interfacial curvature of micelles but reduces intrinsic curvature of membranes

Addition of glycerol has opposite effects on the properties governing intrinsic curvature: It dehydrates the head groups (like increasing T) yet orders the membrane (like decreasing T, see also Fig. 6). The results suggest that head group dehydration dominates the free energy of the detergent (red squares in Fig. 4B, the slope being comparable to temperature increase in Fig. 4D — the abscissae are related by 1 K/v%). In line with other evidence (see introduction), the EO chain at room temperature seems to interact weakly with many water molecules so that it is extraordinarily susceptible to glycerol-induced dehydration. However, the slight decrease of the bilayer-preference of the lipid, qualitatively in line with temperature decrease, suggests that the behavior of the lipid is dominated by the chain ordering effect of glycerol. This ordering effect has been detected as an increase in DPH anisotropy (Fig. 6) or activity to favor the gel phase [13,14]; it results from the increase in interfacial tension of the membrane which is in equilibrium with repulsive forces in the chain and head group regions (principle of opposing forces [48,49,54]) so that the equilibrium area per molecule decreases. Relating the glycerol and temperature effect on the lipid preference, $\Delta\mu_L^{0,m\to b}$, we obtain ~ −0.2 K/v%, which is comparable to the correlation of the effects on DPH dynamics (Fig. 6).

The hydrodynamic radius of the micelle depends on the molecular size (length of the stretched chain and thickness of the hydrated head group layer) and shape (a more positive c_0 causes a micelle with a larger curvature, c, i.e., smaller radius $R = 1/c$). The decrease in hydrodynamic size (Fig. 5) could thus be explained in terms of a reduced thickness of the head group region caused by dehydration. We should, however, mention that the literature suggests also the aggregation number of EO-detergent to be diminished by glycerol [55], which corresponds to a stronger curvature, c, and implies a more positive c_0. It may appear paradoxical that c_0 increases in a micelle but decreases markedly in a membrane but this is not a contradiction. In the spherical geometry of a micelle, the cross-sectional area decreases with decreasing distance from the midpoint so that a relocation of the head group towards the core can, indeed, cause an increased c_0 [55]. In a membrane, the head group repulsion controlling the lateral area per molecule is strongest in a layer somewhat 'above' the hydrophobic–hydrophilic interface. The dehydrated EO-chain can relocate to a less packed region and partially solvate the lipid head group [56,57] (thus freeing water from it, particularly at reduced water activity). This reduces the combined lateral area requirement of the lipid and detergent head groups and relaxes curvature stress.

4.5. Urea renders solvated head groups 'big but soft'

Urea shows a relatively weak, nonlinear effect on lipid–detergent parameters as a consequence of a partial compensation of opposing effects. Up to $\phi_U = 10\%$, urea shifts the preferences of the detergent ($d\Delta\mu_D^{m\to b}/d\phi_U$, Fig. 4A) as well as the lipid (Fig. 4B) somewhat in favor of micelles. Both slopes are 24 J/(mol v%) which correlates with the temperature effect (Fig. 4D,E) by −1.6 K/v%. This is what one should expect given the increased solvation of the head group in the presence of urea, which renders the intrinsic curvature more positive. Such an increase in c_0 is also in line with a shrinking of the micelles (Fig. 5B) and an inhibition of the lamellar-to-inverse hexagonal transition of certain lipids [14,17] caused by urea. However, in contrast to other effects increasing c_0 such as larger head groups of the lipid [58], lower temperature [42], larger EO-head group [42], or decreasing glycerol content (Fig. 4), urea does not increase the enthalpy of bilayer insertion of $C_{12}EO_8$, $\Delta H_D^{m\to b}$ (Fig. 4C), which typically reflects increased curvature strain. Instead, urea renders the enthalpy more favorable while the free energy becomes less favorable. This implies that urea causes a penalty to the entropy of membrane insertion (compared to localization in a micelle). Recalling that there are two types of strains that can result from curvature stress, (i) head group desolvation and compaction and (ii) chain disordering (endothermic, entropically favorable), we may speculate that urea shifts the balance of these two to a more pronounced head group compaction. In other words, the urea and additional water molecules that solvate the head groups are bound only weakly, by a gain in conformational and motional freedom of the head groups (see [59] on entropy-driven hydration of lipids), and render the head group bigger but 'softer' in the presence of urea. This explains also why neither order nor dynamics of DPH reflected a loser packing of the chains in the presence of 2 M (not shown) and 3 M (Fig. 6B) urea. At very high urea, Walter et al. [20] have found the membrane–micelle coexistence range for OG to become very narrow, which implies that the two phases become very similar to each other in terms of the free energy of lipid and detergent. This is, qualitatively, seen also for $C_{12}EO_8$ at 4 M urea (Fig. 4A, B).

4.6. Electrostatics

It should be mentioned that urea and glycerol may affect lipid–detergent interactions also by increasing or decreasing the dielectric

constant of the solvent, respectively, thus attenuating or boosting electrostatic interactions. This is of primary importance for charged lipids or surfactants but may have some influence here as well, because it affects the (repulsive) dipole–dipole interactions between the lipids. In water, the insertion of $C_{12}EO_8$ into POPC vesicles was found to raise the orientation of the head groups, normally largely in-plane with the membrane surface, to a more upright orientation [60]. This relaxes, to some extent, head group packing and positive curvature stress. Urea and glycerol are likely to modify these phenomena but the resulting changes to the insertion of detergents are probably weak and complex and will not be discussed in detail here.

5. Conclusions

1) The effects of cosolvents on association and interaction parameters of lipids and detergents are complex and cannot be understood in terms of the 'salting in' or 'salting out' of solutes due to changes in water structure alone. While these effects contribute to the behaviour of the systems, they may be overcompensated by cosolvent effects on intrinsic curvature and aggregate structure and order.
2) Urea promotes positive intrinsic curvature by facilitating the solvation of the polar head groups. However, the resulting curvature stress is an entropic rather than enthalpic penalty as usual. This may be explained by the strain applying more to the head groups (desolvation, compaction) rather than the chains (disordering).
3) Glycerol dehydrates and contracts the EO-chain. This results in the apparent paradox that intrinsic curvature is increased in micelles (which shrink) but decreased for mixed detergent and lipid in a membrane (opposing membrane solubilization).
4) Glycerol reduces the absolute value of the free energy of transfer of lipid and detergents between micelles and membranes, i.e., it renders membranes and micelles thermodynamically more similar. This tends to improve the homogeneity of the protein distribution in reconstituted proteoliposomes.

Acknowledgements

I, H. H., dedicate this work to Alfred Blume (MLU Halle, Germany) on the occasion of his 65th birthday. I am truly indebted to him for introducing me into the field of calorimetry. I admire particularly his successful, high-risk, self-experiment that has ruled out the widely accepted hypothesis that important science needs barefaced overstatement, pathological vanity, conspiracy, and competitor-paranoia.

We thank Tigran Chalikian, Alekos Tsamaloukas, and Sandro Keller for helpful discussions.

This study was funded by NSERC (grant 341920-07).

References

[1] H. Heerklotz, Interactions of surfactants with lipid membranes, Quarterly Reviews of Biophysics 41 (2008) 205–264.
[2] J. Lasch, Interaction of detergents with lipid vesicles, Biochimica et Biophysica Acta 1241 (1995) 269–292.
[3] A. Alonso, F.M. Goni (Eds.), Detergents in biomembrane studies, Biochimica et Biophysica Acta, 1508 (1–2), 2000, pp. 1–251.
[4] R. Grisshammer, J.F. White, L.B. Trinh, J. Shiloach, Large-scale expression and purification of a G-protein-coupled receptor for structure determination — an overview, Journal of Structural and Functional Genomics 6 (2005) 159–163.
[5] C.G. Tate, R. Grisshammer, Heterologous expression of G-protein-coupled receptors, Trends in Biotechnology 14 (1996) 426–430.
[6] D. Krepkiy, K. Gawrisch, A. Yeliseev, Expression and purification of CB2 for NMR studies in micellar solution, Protein and Peptide Letters 14 (2007) 1031–1037.
[7] R.L. Rich, A.R. Miles, B.K. Gale, D.G. Myszka, Detergent screening of a G-protein-coupled receptor using serial and array biosensor technologies, Analytical Biochemistry 386 (2009) 98–104.
[8] A.A. Yeliseev, K.K. Wong, O. Soubias, K. Gawrisch, Expression of human peripheral cannabinoid receptor for structural studies, Protein Science 14 (2005) 2638–2653.
[9] A. Beck, A.D. Tsamaloukas, P. Jurcevic, H. Heerklotz, Additive Action of Two or More Solutes on Lipid Membranes, Langmuir, 2008.
[10] K. Gekko, S.N. Timasheff, Mechanism of protein stabilization by glycerol: preferential hydration in glycerol–water mixtures, Biochemistry 20 (1981) 4667–4676.
[11] S.N. Timasheff, The control of protein stability and association by weak interactions with water: how do solvents affect these processes? Annual Review of Biophysics and Biomolecular Structure 22 (1993) 67–97.
[12] N. Smolin, R. Winter, Effect of temperature, pressure, and cosolvents on structural and dynamic properties of the hydration shell of SNase: a molecular dynamics computer simulation study, Journal of Physical Chemistry B 112 (2008) 997–1006.
[13] P. Westh, Unilamellar DMPC vesicles in aqueous glycerol: preferential interactions and thermochemistry, Biophysical Journal 84 (2003) 341–349.
[14] R. Koynova, J. Brankov, B. Tenchov, Modulation of lipid phase behavior by kosmotropic and chaotropic solutes. Experiment and thermodynamic theory, European Biophysics Journal 25 (1997) 261–274.
[15] W.P. Williams, P.J. Quinn, L.I. Tsonev, R.D. Koynova, The effects of glycerol on the phase behaviour of hydrated distearoylphosphatidylethanolamine and its possible relation to the mode of action of cryoprotectants, Biochimica et Biophysica Acta — Biomembranes 1062 (1991) 123–132.
[16] M. Bryszewska, R.M. Epand, Effects of sugar alcohols and disaccharides in inducing the hexagonal phase and altering membrane properties: Implications for diabetes mellitus, Biochimica et Biophysica Acta — Biomembranes 943 (1988) 485–492.
[17] P.W. Sanderson, L.J. Lis, P.J. Quinn, W.P. Williams, The Hofmeister effect in relation to membrane lipid phase stability, Biochimica et Biophysica Acta — Biomembranes 1067 (1991) 43–50.
[18] K. Aramaki, U. Olsson, Y. Yamaguchi, H. Kunieda, Effect of water-soluble alcohols on surfactant aggregation in the C12EO8 system, Langmuir 15 (1999) 6226–6232.
[19] G. D'Errico, D. Ciccarelli, O. Ortona, Effect of glycerol on micelle formation by ionic and nonionic surfactants at 25 °C, Journal of Colloid and Interface Science 286 (2005) 747–754.
[20] A. Walter, G. Kuehl, K. Barnes, G. VanderWaerdt, The vesicle-to-micelle transition of phosphatidylcholine vesicles induced by nonionic detergents: effects of sodium chloride, sucrose and urea, Biochimica et Biophysica Acta 1508 (2000) 20–33.
[21] C.C. Ruiz, F.G. Sanchez, Effect of urea on aggregation behavior of Triton X-100 micellar solutions: a photophysical study, Journal of Colloid and Interface Science 165 (1994) 110–115.
[22] Y. Feng, Z.W. Yu, P.J. Quinn, Effect of urea, dimethylurea, and tetramethylurea on the phase behavior of dioleoylphosphatidylethanolamine, Chemistry and Physics of Lipids 114 (2002) 149–157.
[23] S.K. Patra, A. Alonso, F.M. Goni, Detergent solubilisation of phospholipid bilayers in the gel state: the role of polar and hydrophobic forces, Biochimica et Biophysica Acta 1373 (1998) 112–118.
[24] C. McKibbin, N.A. Farmer, P.C. Edwards, C. Villa, P.J. Booth, Urea unfolding of opsin in phospholipid bicelles, Photochemistry and Photobiology 85 (2009) 494–500.
[25] G.C. Kresheck, W.A. Hargraves, Thermometric titration studies of the effect of head group, chain length, solvent, and temperature on the thermodynamics of micelle formation, Journal of Colloid and Interface Science 48 (1974) 481–493.
[26] G. Olofsson, Microtitration calorimetric study of the micellization of three poly (oxyethylene) glycol dodecyl ethers, Journal of Physical Chemistry 89 (1985) 1473–1477.
[27] S. Paula, W. Süs, J. Tuchtenhagen, A. Blume, Thermodynamics of micelle formation as a function of temperature: a high sensitivity titration calorimetry study, Journal of Physical Chemistry 99 (1995) 11742–11751.
[28] H. Heerklotz, R.M. Epand, The enthalpy of acyl chain packing and the apparent water-accessible apolar surface area of phospholipids, Biophysical Journal 80 (2001) 271–279.
[29] A.D. Tsamaloukas, S. Keller, H. Heerklotz, Uptake and release protocol for assessing membrane binding and permeation by way of isothermal titration calorimetry, Nature Protocols 2 (2007) 695–704.
[30] H. Heerklotz, A. Tsamaloukas, S. Keller, Monitoring detergent-mediated solubilization and reconstitution of lipid membranes by isothermal titration calorimetry, Nature Protocols 4 (2009) 686–697.
[31] K. Kiyosawa, Volumetric properties of polyols (ethylene–glycol, glycerol, meso-erythritol, xylitol and mannitol) in relation to their membrane-permeability — group additivity and estimation of the maximum radius of their molecules, Biochimica et Biophysica Acta 1064 (1991) 251–255.
[32] K. Nakanishi, Partial molal volumes of butyl alcohols and of related compounds in aqueous solution, Bulletin. Chemical Society of Japan 33 (1960) 793–797.
[33] R.C. MacDonald, R.I. MacDonald, B.P. Menco, K. Takeshita, N.K. Subbarao, L.R. Hu, Small-volume extrusion apparatus for preparation of large, unilamellar vesicles, Biochimica et Biophysica Acta 1061 (1991) 297–303.
[34] H. Heerklotz, J. Seelig, Titration calorimetry of surfactant–membrane partitioning and membrane solubilization, Biochimica et biophysica Acta 1508 (2000) 69–85.
[35] H.H. Heerklotz, H. Binder, R.M. Epand, A "release" protocol for isothermal titration calorimetry, Biophysical Journal 76 (1999) 2606–2613.
[36] A. Tsamaloukas, H. Heerklotz, Uptake and release protocol for assessing membrane binding and permeation by way of isothermal titration calorimetry, Nature Protocols 2 (2007) 695–704.
[37] D. Lichtenberg, Characterization of the solubilization of lipid bilayers by surfactants, Biochimica et Biophysica Acta 821 (1985) 470–478.
[38] G. Beschiaschvili, J. Seelig, Peptide binding to lipid bilayers. Nonclassical hydrophobic effect and membrane-induced pK shifts, Biochemistry 31 (1992) 10044–10053.

[39] A. Helenius, K. Simons, Solubilization of membranes by detergents, Biochimica et Biophysica Acta 415 (1975) 29–79.
[40] H. Heerklotz, G. Lantzsch, H. Binder, G. Klose, A. Blume, Application of isothermal titration calorimetry for detecting lipid membrane solubilization, Chemical Physics Letters 235 (1995) 517–520.
[41] H. Heerklotz, G. Lantzsch, H. Binder, G. Klose, A. Blume, Thermodynamic characterization of dilute aqueous lipid/detergent mixtures of POPC and C12EO8 by means of isothermal titration calorimetry, Journal of Physical Chemistry 100 (1996) 6764–6774.
[42] H. Heerklotz, H. Binder, G. Lantzsch, G. Klose, A. Blume, Lipid/detergent interaction thermodynamics as a function of molecular shape, Journal of Physical Chemistry B 101 (1997) 639–645.
[43] F.O. Costa-Balogh, H. Wennerstrom, L. Wadso, E. Sparr, How small polar molecules protect membrane systems against osmotic stress: The urea–water–phospholipid system, Journal of Physical Chemistry B 110 (2006) 23845–23852.
[44] S. Kumar, N. Parveen, D. Kabir Ud, Effect of urea addition on micellization and the related phenomena, Journal of Physical Chemistry B 108 (2004) 9588–9592.
[45] A. Nicholls, K.A. Sharp, B. Honig, Protein folding and association: insights from the interfacial and thermodynamic properties of hydrocarbons, Proteins: Structure, Function and Genetics 11 (1991) 281–296.
[46] E. Tuchsen, M.A. Jensen, P. Westh, Solvent accessible surface area (ASA) of simulated phospholipid membranes, Chemistry and Physics of Lipids 123 (2003) 107–116.
[47] J.K. Myers, C.N. Pace, J.M. Scholtz, Denaturant m values and heat capacity changes: relation to changes in accessible surface areas of protein unfolding, Protein Science 4 (1995) 2138–2148.
[48] J.N. Israelachvili, Intermolecular and surface forces, Academic press, London, 1991.
[49] J.N. Israelachvili, S. Marcelja, R.G. Horn, Physical principles of membrane organization, Quarterly Reviews of Biophysics 13 (1980) 121–200.
[50] D. Andelman, M.M. Kozlov, W. Helfrich, Phase-transitions between vesicles and micelles driven by competing curvatures, Europhysics Letters 25 (1994) 231–236.
[51] W. Helfrich, Elastic properties of lipid bilayers — theory and possible experiments, Zeitschrift Fur Naturforschung C-a Journal of Biosciences C 28 (1973) 693–703.
[52] H. Heerklotz, J. Seelig, Correlation of membrane/water partition coefficients of detergents with the critical micelle concentration, Biophysical Journal 78 (2000) 2435–2440.
[53] M.M. Kozlov, D. Andelman, Theory and phenomenology of mixed amphiphilic aggregates, Current Opinion in Colloid & Interface Science 1 (1996) 362–366.
[54] G. Cevc, D. Marsh, Phospholipid Bilayers, John Wiley and Sons, New York, 1985.
[55] J.M. Hierrezuelo, J.A. Molina-Bolivar, C.C. Ruiz, On the urea action mechanism: a comparative study on the self-assembly of two sugar-based surfactants, Journal of Physical Chemistry B 113 (2009) 7178–7187.
[56] M.J. Schneider, S.E. Feller, Molecular dynamics simulations of a phospholipid–detergent mixture, Journal of Physical Chemistry B 105 (2001) 1331–1337.
[57] F. Volke, A. Pampel, Membrane hydration and structure on a subnanometer scale as seen by high resolution solid state nuclear magnetic resonance: POPC and POPC/C12EO4 model membranes, Biophysical Journal 68 (1995) 1960–1965.
[58] R.M. Epand, R.F. Epand, Calorimetric detection of curvature strain in phospholipid bilayers, Biophysical Journal 66 (1994) 1450–1456.
[59] H. Binder, B. Kohlstrunk, H.H. Heerklotz, Hydration and lyotropic melting of amphiphilic molecules: a thermodynamic study using humidity titration calorimetry, Journal of Colloid and Interface Science 220 (1999) 235–249.
[60] H. Heerklotz, T. Wieprecht, J. Seelig, Membrane perturbation by the lipopeptide surfactin and detergents as studied by deuterium NMR, Journal of Physical Chemistry B 108 (2004) 4909–4915.